



## **Effects of Shear on the Elastic Lateral Torsional Buckling of Singly-Symmetric I-beams**

Xiaoyi Chen<sup>1\*</sup>, Chen Liang<sup>2\*</sup>, Todd Helwig<sup>3</sup>

### **Abstract**

Previous studies have shown that the elastic lateral torsional buckling (LTB) of doubly-symmetric I-beams can be significantly affected by web shear. Design solutions were recommended in these previous investigations, but the applicability to singly-symmetric girders was not investigated. This paper outlines a numerical study on the impact of shear on the LTB behavior of singly-symmetric I-beams. Eigenvalue buckling analyses were conducted to compare the LTB capacity of fully-stiffened, partially-stiffened, and unstiffened beams with webs subjected to cases with both constant shear and shear gradient. Numerical parametric studies were conducted to investigate the effects of web slenderness ratio, unbraced length-to-depth ratio and ratio of area of top to bottom flange on the LTB resistance. The effects of nonlinear geometry on the LTB capacity were also studied through large-displacement analyses. The feasibility of proposed design methods developed for doubly-symmetric I-beams that account for the reduction of LTB capacity due to shear were investigated for singly-symmetric I-beams.

### **1. Introduction**

Lateral torsional buckling (LTB) is a structural stability limit state when the steel beams are subjected to bending moments. The LTB involves both lateral displacement and twist of a steel beam that leads to instability. The LTB limit state is often critical to ensure steel stability and should be carefully considered in the design of steel structures. Theoretical solutions to determine the critical LTB capacity of steel beams (Timoshenko and Gere 1961; Galambos 1968), which are presented in detail later, form a solid basis for the modern design methods of steel beams. The theoretical solutions assume a rigid web cross-section, which can be violated for slender beams. There has been a growing emphasis on accounting for the effects of web distortion in the estimation of elastic LTB resistance of steel beams.

Previous studies (Bradford and Trahair 1981; Bradford 1985; Bradford 1992) have shown the negative effects of web distortion on the LTB resistance, which refers to the phenomenon of the lateral distortional buckling (LDB). LDB is a mode of stability involving the interaction between

---

<sup>1</sup> Postdoctoral fellow, University of Texas at Austin, [xiaoyi.chen@utexas.edu](mailto:xiaoyi.chen@utexas.edu)

<sup>2</sup> Postdoctoral fellow, Tongji University, [liangchen1201@tongji.edu.cn](mailto:liangchen1201@tongji.edu.cn)

<sup>3</sup> Jewel McAlister Smith Professor in Engineering, University of Texas at Austin, [thelwig@mail.utexas.edu](mailto:thelwig@mail.utexas.edu)

\* Indicates equal contribution

LTB and web local buckling, which may occur when beams are subjected to either uniform moment (zero shear) or moment gradient.

In the case of beams subjected to moment gradient, the effects of shear along the unbraced length may also reduce the LTB capacity of steel beams. This mode of instability involves the interaction between LTB and web shear buckling. A limited number of investigations have been conducted to study the effects of web shear on the elastic LTB resistance of steel beams. Bradford (1992) numerically investigated the elastic LTB resistance of cantilever beams and noticed that the LTB resistance was significantly affected by web distortion, particularly for short beams with slender webs. The study conducted by Moore (1995) confirmed the reduction of LTB resistance due to shear and indicated that the LTB resistance was negatively affected when the shear exceeded 30% of the shear capacity. Liang et al. (2022) investigated the effects of shear on the elastic LTB of doubly-symmetric I-beams under various loading conditions through computational models considering a wide range of geometries. The LTB resistance was significantly reduced due to the shear effects and the reduction of LTB was more obvious for webs with higher values of the slenderness ratio. Phillips et al. (2023) investigated the reduction effects of web shear on the LTB capacity through experimental testing.

The effects of web distortion are considered in the design equation of LTB of current design specifications (AASHTO 2020; AISC 2016) based on Winter's approach (Winter 1943) by neglecting the St. Venant torsional constant ( $J$ ) for slender webs. The effects of shear on the LTB resistance are not considered in current design specifications. However, the numerical investigation by Liang et al. (2022) indicated that the reduction of the elastic LTB resistance was dependent on the magnitude of the applied shear relative to the shear buckling capacity. As a result, Winter's approach tends to underestimate the LTB resistance when the shear is relatively small and overestimate the LTB when the shear is relatively large. Based on numerical findings, practical design methods were proposed to determine the elastic LTB resistance for doubly-symmetric I-beams by incorporating a moment reduction factor to account for shear effects.

Despite valuable insights provided by previous studies, the effects of shear on the LTB resistance are not thoroughly investigated and well-established in design specifications. Although singly-symmetric sections are commonly used in buildings and bridges, relatively few studies have been conducted on the effects of shear in these girders. This paper documents a numerical study on the effects of shear on the elastic LTB resistance of singly-symmetric I-beams. A brief overview of the design equations relevant to the elastic LTB of steel beams is first presented. A numerical parametric study is presented to discuss the LTB behavior of singly-symmetric beams with various geometries. The feasibility of proposed design equations developed for doubly-symmetric I-beams, which is practical by incorporating a moment reduction factor for the elastic LTB resistance due to shear effects, is investigated for singly-symmetric I-beams.

## **2. Background**

### *2.1 Elastic LTB resistance*

Current design specifications (AASHTO 2020; AISC 2016) recommend design equations for the LTB resistance of steel beams based on classic theoretical solutions with a moment gradient factor. Theoretical solutions for the elastic LTB of beams under uniform moment loading are summarized as follows:

- For doubly-symmetric beams, the theoretical solution,  $M_{cr,th}$ , is given by Eq. 1 (Timoshenko and Gere 1961):

$$M_{cr,th} = \frac{\pi}{L_b} \sqrt{EI_y GJ + \left(\frac{\pi E}{L_b}\right)^2 I_y C_w} \quad (1)$$

- For singly-symmetric beams, the theoretical solution,  $M_{cr,th}$ , is given by Eqs. 2 and 3 which assume no web distortion (Galambos 1968):

$$M_{cr,th} = \frac{\pi^2 EI_y}{L_b^2} \left[ \frac{\beta_x}{2} + \sqrt{\left(\frac{\beta_x}{2}\right)^2 + \left(\frac{C_w}{I_y} + \frac{GJ}{EI_y} \frac{I_b^2}{\pi^2}\right)} \right] \quad (2)$$

$$\beta_x = \frac{1}{I_x} \int_A y(x^2 + y^2) dA - 2y_o \quad (3)$$

where  $L_b$  is the unbraced length;  $I_y$  is the second moment of area about the weak axis;  $E$  is the modulus of elasticity;  $G$  is the elastic shear modulus;  $J$  is the St. Venant constant; and  $C_w$  is the warping constant. Specifically for singly symmetric beams,  $I_x$  is the second moment of area about the strong axis, and  $y_o$  is the distance between the shear center and the centroid of the section.

To account for the effects of moment gradient along the unbraced length, a moment gradient factor  $C_b$  is typically multiplied with the theoretical solution of the elastic LTB for beams under uniform loading to estimate the buckling capacity of beams subjected to variable moment. The moment gradient factor,  $C_b$ , can be estimated using Eqs. 4 and 5 for singly-symmetric sections (Helwig et al. 1997; Reichenbach et al. 2020):

$$C_b = \left( \frac{12.5M_{\max}}{2.5M_{\max} + 3M_A + 4M_B + 3M_C} \right) R_m \leq 3.0 \quad (4)$$

$$R_m = \begin{cases} 0.5 + 2 \left( \frac{I_{y, \text{top}}}{I_y} \right)^2, & \text{reverse-curvature bending} \\ 1.0, & \text{single-curvature bending} \end{cases} \quad (5)$$

where  $M_A$ ,  $M_B$ , and  $M_C$  are the moments at quarter point, centerline, and the three-quarter point of the unbraced length, respectively;  $M_{\max}$  is the maximum moment within the unbraced length;  $I_{y, \text{top}}$  is the second moment of area of the top flange about the weak axis.

## 2.2 Moment reduction factor on LTB due to shear by Liang et al. (2022)

Liang et al. (2022) proposed practical design methods to determine the elastic LTB resistance  $M_{cr}$  for doubly-symmetric I-beams based on findings from a comprehensive numerical parametric study, as shown in Eq. 6.  $M_{cr,th}$  is the theoretical elastic LTB resistance for doubly-symmetric beams subjected to uniform moment loading as shown in Eq. 1, and  $C_b$  is the moment gradient factor as shown in Eqs. 4 and 5.  $C_{mv}$  is the newly-proposed factor to account for the LTB reduction due to shear effects, which is given by Eqs. 7 and 8:

$$M_{cr} = C_{mv} C_b M_{cr,th} \quad (6)$$

$$C_{mv} = \frac{V_{cr,th}}{V_{cr,th} + \alpha V_{st}} \quad (7)$$

$$\alpha = 0.11 C_b \sqrt{A_w / A_f} \quad (8)$$

where  $V_{cr,th}$  is the theoretical solution for the critical shear buckling capacity of either unstiffened or stiffened webs (Timoshenko and Gere, 1961);  $V_{st}$  is the shear corresponding to the theoretical elastic LTB resistance estimated by  $C_b M_{cr,th}$  without considering reduction due to shear; and  $A_w$  and  $A_f$  are the areas of web and a single flange, respectively. The proposed method is applicable for beams subjected to either a constant shear or shear gradient. In the case of a shear gradient,  $V_{st}$  can be taken as the average shear values at two ends of the unbraced segment.

### 3. Development of the Finite Element Model

Numerical finite element (FE) models of singly-symmetric steel beams were modeled using the commercial software Abaqus (Systèmes 2020). Two types of analyses were conducted in the present study: 1) eigenvalue buckling analyses to determine the LTB capacity of beams with various geometric features under different loading conditions; 2) large-displacement analyses with nonlinear geometry and initial imperfections.

#### 3.1 Description of the modeling strategy

Fig. 1 depicts the schemes of the FE model with different levels of stiffening depending on the ratio of the stiffener spacing to web depth. The unstiffened model has no stiffeners along the length of the beam, whereas the fully-stiffened model has a stiffener spacing to depth ratio of 0.25. It is reasonably deemed that the fully-stiffened beam is exempt from effects of web distortion associated with shear effects. Increasing the stiffener spacing ratio significantly above 0.25, results in partially-stiffened model, which results in a reduction in the shear-buckling capacity compared to fully-stiffened beams. The web stiffeners were modeled with a gap of 2.54 mm (0.1") to both flanges to avoid warping restraints, as depicted in Fig. 1. The webs and the flanges of beams were simulated using four-node shell elements designated as S4R available in Abaqus. Upon a sensitivity analysis of mesh size, it was deemed reasonable to utilize a global mesh size of approximately 25.4 mm (1"). Linear elastic material properties were utilized for both eigenvalue buckling analyses and large-displacement analyses. For Grade 50 steel, the yield strength was taken as 345 MPa (50 ksi).

The boundary conditions are illustrated on an unstiffened beam model, as shown in Fig. 1. The simply-supported boundary conditions were imposed at both ends of the beam. The vertical translational movements at the mid-height of the cross-section at both ends were restrained as well. The lateral translational movements were restrained along the web at both ends and the brace points for stiffened models as well. As a result, the imposed boundary conditions restrained twist but allowed warping at the ends of the beam. The assumption of free warping at braced points used in this study is consistent with the current design specifications.

Uniformly distributed loads (UDL) along the length of the beam were applied at the mid-height of the cross-section to represent self-weight of the beam. Although the self-weight was applied above the geometric centroid of singly-symmetric beams, it was deemed reasonable to neglect the effects

of load position based on previous findings (Helwig et al. 1997). In addition, various moment loading conditions were considered, resulting in zero shear, constant shear and shear gradient along the unbraced length. For both ends of the beam, force couples were uniformly applied at top and bottom flanges to impose various moment and shear gradient along the unbraced length.

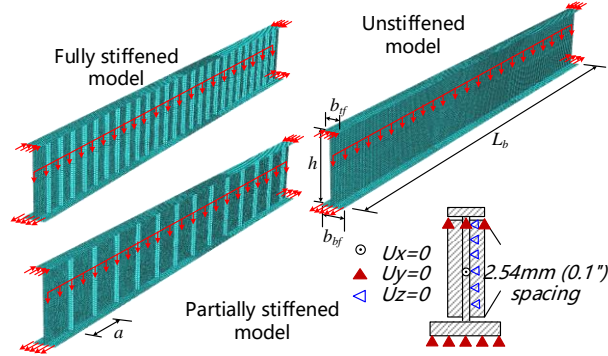


Figure 1: FE model in the parametric study.

### 3.2 An overview of geometric parameters

For singly symmetric beams, the degree of mono-symmetry is defined by a parameter,  $\rho_{top} = I_{y_{top}}/I_y$ , where  $I_{y_{top}}$  is the second moment of area of the top flange about an axis through the web, and  $I_y$  is the second moment of area of the section about the same axis. In the present study, the cross-sections varied to have a degree of mono-symmetry in the range of 0.1 and 0.5. The lower bound of this range ( $\rho_{top} = 0.1$ ) corresponds to the limit value as specified in AASHTO Article 6.10.2.2 (AASHTO 2020) that  $\rho_{top}$  should be larger than 0.091, and the upper bound (0.5) corresponds to a doubly-symmetric section. The value of  $\rho_{top}$  exceeding 0.5, corresponding to singly-symmetric beam sections with a smaller bottom flange than the top flange, was not considered in the present study considering that sections with smaller top flanges are more common in the structural field. However, the findings from the present study should provide insight on the LTB behavior for singly symmetric beams with a value of  $\rho_{top}$  exceeding 0.5. The unbraced length-to-depth ratio varied as values of 6.7, 10, 15, and 20.

Table 1 summarizes the parameters and corresponding values considered in the present study. All cross-sections were prismatic along the unbraced length. The parametric studies considered beam sections with a constant web height of 914 mm (36"), and a constant top flange of 152.4mm×12.7mm (6"× 0.5"). The cross-sections of the bottom flange were changed to achieve various degrees of mono-symmetry. In total, eight dimensions of the bottom flange were considered. The resulting depth-to-flange width ratio ( $h/b_f$ ) for the bottom flange varied from 3.4 corresponding to typical rolled I-shaped sections, to 6 corresponding to the limit as specified in AASHTO (AASHTO 2020). The top flange had a constant depth-to-flange width ratio of 6. The top flange had a constant width-to-thickness ratio ( $b_f/t_f$ ) of 12, and for the bottom flange, this ratio varied from 6 to 18, which satisfied the definitions of compact flanges for Grade 50 steel to prevent local buckling of the flanges (AISC 2016). The web slenderness ratio ( $h/t_w$ ) varied in a relatively large range of 30 to 250, including compact, non-compact and slender webs to investigate its effects on the LTB resistance.

Table 1: Geometric parameters of the FE models.

Parameter	Value
Stiffener spacing-to-depth ratio ( $a/h$ )	0.25(Fully stiffened), 0.5-3.4(partially stiffened), unstiffened
Unbraced length-to-depth ratio ( $L_b/h$ )	6.7; 10; 15; 20
Depth-to-flange width ratio ( $h/b_f$ )	6.0 (top flange, $h/b_{tf}$ ); 3.4-6.0 (bottom flange, $h/b_{bf}$ )
Width-to-thickness ratio of flange ( $b_f/t_f$ )	12 (top flange $b_{tf}/t_{tf}$ ); 6-18 (bottom flange $b_{bf}/t_{bf}$ )
Geometric web slenderness ratio ( $h/t_w$ )	30; 36; 58; 100; 125; 150; 200; 250
Degree of mono-symmetry ( $\rho_{top}$ )	0.10; 0.16; 0.23; 0.29; 0.33; 0.34; 0.40; 0.50
Sizes of top flange ( $b_{tf} \times t_{tf}$ )	152.4mm $\times$ 12.7mm (6" $\times$ 0.5")
Sizes of bottom flange ( $b_{bf} \times t_{bf}$ )	$b_{tf} \times t_{tf}$ ; 1.25 $b_{tf} \times t_{tf}$ ; 1.5 $b_{tf} \times t_{tf}$ ; $b_{tf} \times 1.5t_{tf}$ ; $b_{tf} \times 2t_{tf}$ ; 1.25 $b_{tf} \times 1.25t_{tf}$ ; 1.5 $b_{tf} \times 1.5t_{tf}$ ; 1.75 $b_{tf} \times 1.75t_{tf}$

### 3.3 Types of analysis

Two types of analyses were conducted in the present study. First, eigenvalue buckling analyses were performed under unit load until the occurrence of the LTB, and the critical LTB moment was determined. Second, the large-displacement analyses were conducted with nonlinear geometry and imperfections. The imperfections were determined by first conducting a linear eigenvalue buckling analysis to obtain the eigenvector displacement results of all nodes corresponding to the first buckling mode. An Abaqus/Standard analysis was then conducted with the displacement results of the first eigenvector imported to the model with the maximum value of the imported imperfection set to a value of  $L_b/1000$ , where  $L_b$  is the length between braced points. The imperfection value was deemed representative of typical fabrication tolerances on out-of-straightness.

### 3.4 Model validation

The developed FE models of singly-symmetric beams were validated by comparing the results with the theoretical solutions. According to Eq. 2, the theoretical elastic LTB capacity ( $M_{cr,th}$ ) of singly-symmetric I-beams under the uniform moment loading can be determined. The theoretical solution assumes that the web has a rigid cross-section without distortion under the bending moment. To ensure a valid comparison between the FE results and the theoretical solution, fully-stiffened beams with closely spaced braces ( $a/h = 0.25$ ) to prevent web distortion were modeled and compared against the theoretical method. The eigenvalue buckling analyses were conducted for multiple beams with various bottom flange sizes, web thicknesses, and unbraced length-to-depth ratio. Correspondingly, the critical LTB moments obtained by the FE modeling were designated as  $M_{cr,st,FE}$ , where the subscript "st" represents "full stiffened" sections. The results are shown as the normalized LTB resistance obtained from the FE modeling by the theoretical solution,  $M_{cr,st,FE}/M_{cr,th}$ . Fig. 2 summarizes the normalized results for different values of degree of mono-symmetry.

The normalized numerical LTB capacities have an average value of 0.99 and a standard deviation of 0.017. The maximum difference between the FE result and the theoretical solution was approximately 7%. Overall, the results from FE analyses generally agreed well with the theoretical solutions and the differences were acceptable based on previous analyses (Liang et al. 2022; Reichenbach et al. 2020). Therefore, the proposed FE models for singly-symmetric beams were validated and employed for following parametric studies.

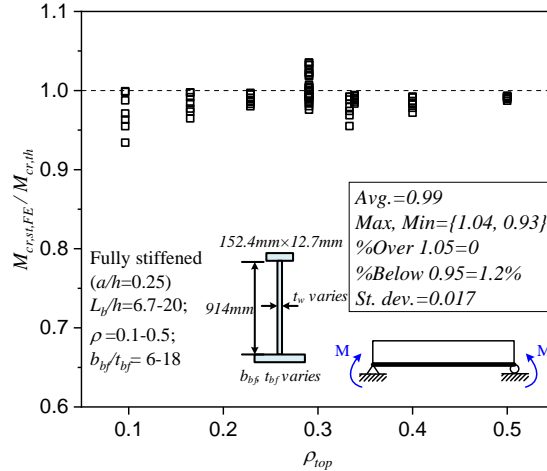


Figure 2: Model validation on stiffened girder subjected to uniform moment.

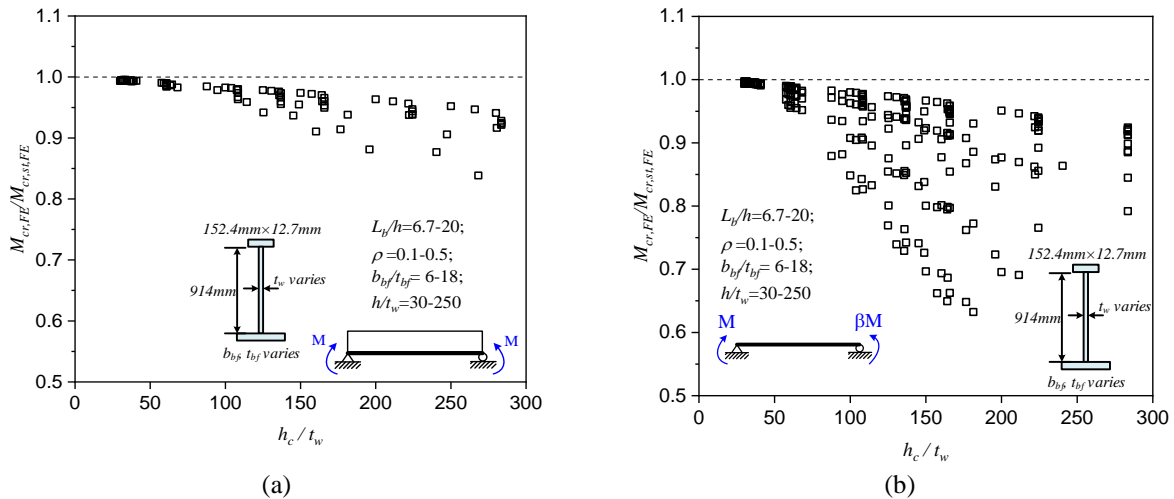
#### 4. Numerical parametric Studies

The effects of shear on the elastic LTB resistance were investigated on the unstiffened beams using the validated FE modeling strategy. Three moment loading conditions were considered: 1) uniform-moment loading, leading to zero shear along the unbraced length; 2) linearly-distributed moment, leading to constant shear, with  $\beta$  indicating the ratio between two end moments ( $\beta = 1, 0.5, 0, -0.5, -1$ ); and 3) moment gradient, leading to linearly-distributed shear.

The LTB resistance of the unstiffened beams obtained by conducting eigenvalue buckling analyses,  $M_{cr,FE}$ , were compared with that of the fully-stiffened beams,  $M_{cr,st,FE}$ . The results are shown as the normalized buckling moment of the unstiffened beams by the buckling moment of the fully stiffened beams, which is denoted as  $M_{cr,FE}/M_{cr,st,FE}$  to indicate the deduction of the LTB resistance due to the shear effects.

##### 4.1 Effects of effective web slenderness ratio ( $h_c/t_w$ )

Fig. 3 presents the effects of effective web slenderness ratio ( $h_c/t_w$ ) on the normalized LTB capacity of unstiffened beams under different loading conditions.



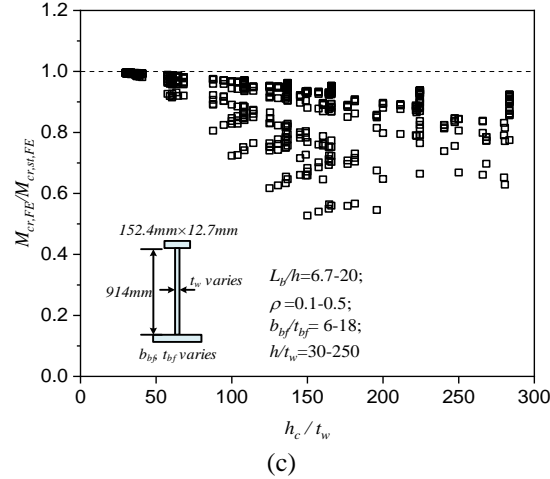
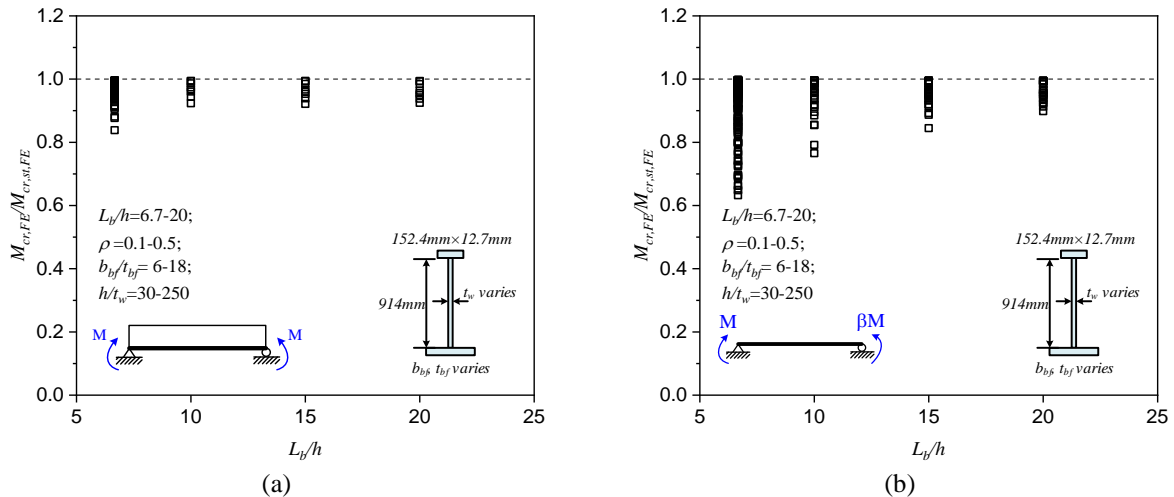


Figure 3: Effects of web slenderness ratio under: (a) zero shear; (b) constant shear; (c) shear gradient.

In the case of a zero shear, as depicted in Fig. 3(a), the reduction in the elastic LTB resistance was more significant as the web slenderness ratio increased, which is likely due to larger web distortion effects for slender webs. This trend was generally true for conditions of constant shear and shear gradient, as shown in Figs. 3(b) and (c). In addition, a higher magnitude of the shear along the unbraced length resulted in a larger reduction in the LTB moment. In the case of zero shear, the moment reduction was approximately 15% for the most slender web. In the case of constant shear, the maximum reduction of the LTB capacity was approximately 35%. In the case of shear gradient, the reduction of the LTB capacity was as large as 45%.

#### 4.2 Effects of unbraced length-to-depth ratio ( $L_b/h$ )

Fig. 4 presents the effects of unbraced length-to-depth ratio ( $L_b/h$ ) on the normalized LTB capacity of unstiffened beams under different loading conditions. A general observation was that the LTB moment of unstiffened beams was less affected by the effects of shear for a smaller value of unbraced length-to-depth ratio. Particularly for cases of constant shear and shear gradient, a decrease in the unbraced length-to-depth ratio efficiently decreased the reduction of LTB moment due to shear. Similar to the observations in Fig. 3, for a certain value of unbraced length-to-depth ratio, the reduction in the LTB moment was increased as the magnitude of the shear increased.





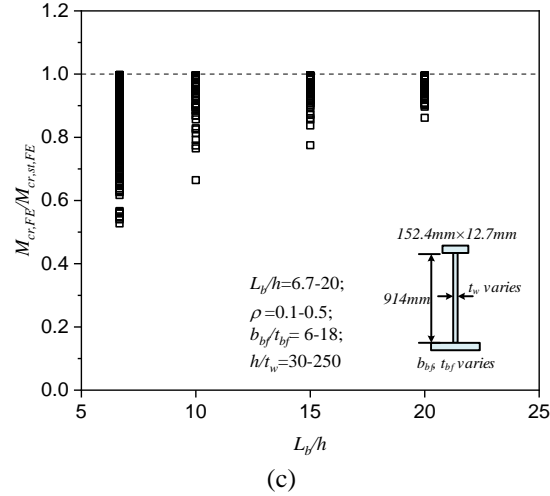


Figure 4: Effects of unbraced length-to-depth ratio under: (a) zero shear; (b) constant shear; (c) shear gradient.

#### 4.3 Effects of ratio of top to bottom flange area ( $A_{tf}/A_{bf}$ )

Fig. 5 presents the effects of ratio of the top flange area to the bottom flange area ( $A_{tf}/A_{bf}$ ) on the normalized LTB capacity of unstiffened beams under different loading conditions.

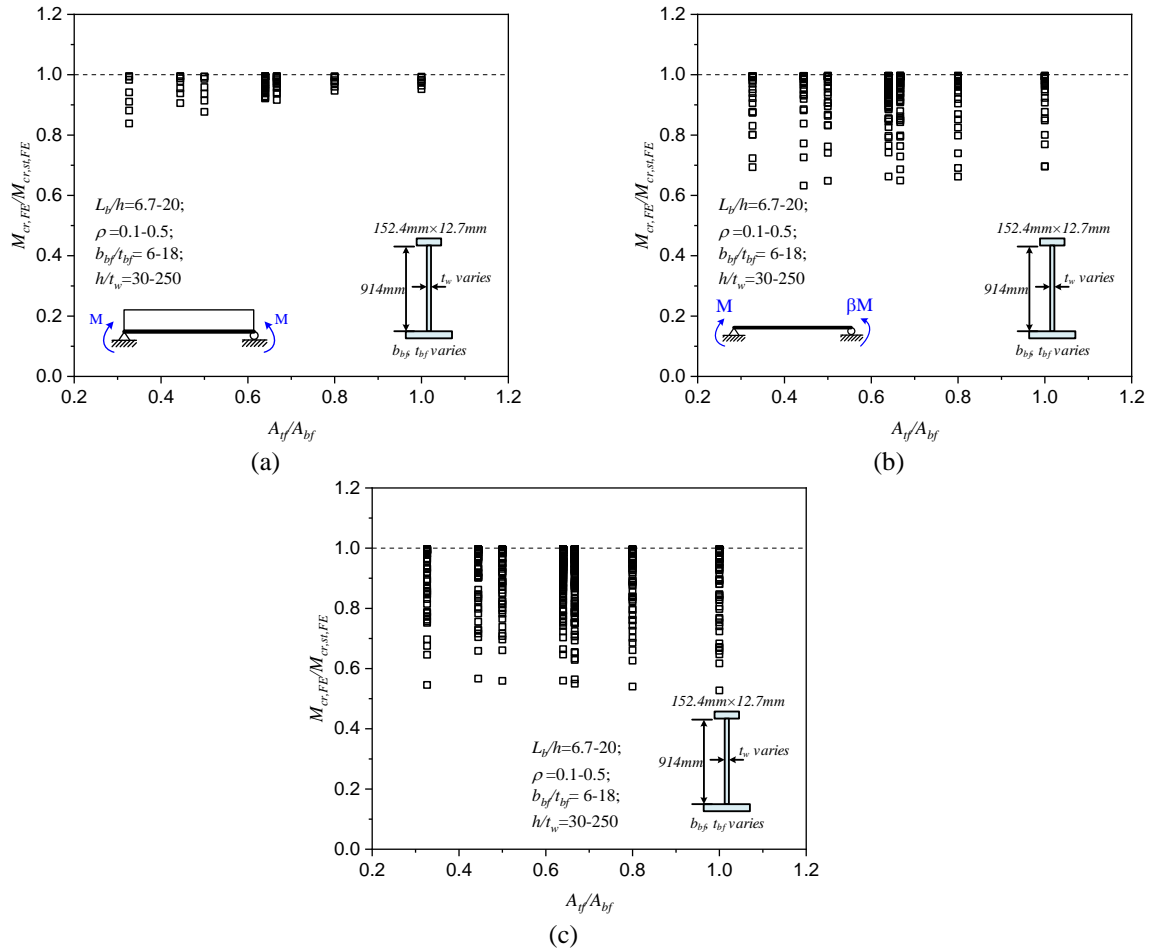


Figure 5: Effects of ratio of top to bottom flange area under: (a) zero shear; (b) constant shear; (c) shear gradient.

A value of 1.0 for  $A_{tf}/A_{bf}$  corresponded to doubly-symmetric beams, and a value smaller than 1.0 corresponded to singly-symmetric beams considered in this study with a smaller top flange compared to bottom flange. It was found that the effect of shear on the LTB behavior was not significantly affected by the ratio of top to bottom flange area.

#### 4.4 Effects of post-buckling strength

Previous studies indicated that the shear strength can significantly increase during the post-buckling period (Daley et al. 2017). Therefore, large-displacement analyses were conducted to evaluate the effects of post-buckling strength by considering nonlinear geometry and imperfections. The selected beams had a constant unbraced length-to-depth ratio of 6.7, a constant web slenderness ratio of 125, whereas the degree of mono-symmetry varied in the range of 0.1 and 0.5 by changing the dimensions of the bottom flange. The analyses were conducted under linearly-distributed moment with three values of  $\beta$ : 1, 0 and -1, for which the magnitude of uniform shear increased correspondingly. For beams with imperfections in the geometry, the critical LTB moment was taken as the moment when the section at the mid-span of the beam twisted a 0.1 rad (Liang et al. 2022).

Fig. 6 plots the effects of nonlinear geometry with variations in the degree of mono-geometry. The moment reductions from the eigenvalue analysis and large-displacement analysis were noted with the solid and open symbols, respectively, in Fig. 6. It was found that with the post-buckling strength, the LTB moment reduction due to shear was slightly lower for unstiffened beams. The benefits of the post-buckling strength were more obvious when the beams were subjected to a relatively larger uniform shear along the unbraced length. In addition, a larger reduction in the LTB moment was observed for beams with lower degree of mono-symmetry.

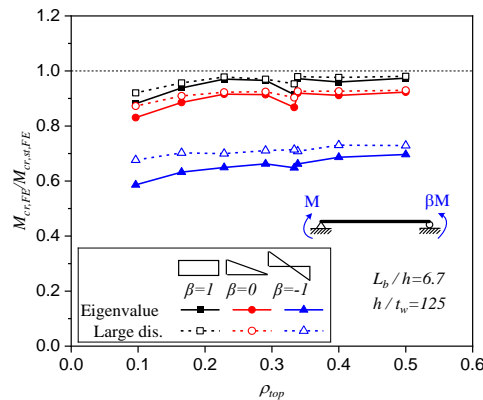


Figure 6: Effects of nonlinear geometry with variations in degree of mono-symmetry.

## 5. Evaluation of design equations

The accuracy of previously proposed equations for doubly-symmetric I-beams (Eqs. 6-8) by incorporating a moment reduction factor to account for the effects of shear was evaluated with the results from eigenvalue analyses and large-displacement analyses for singly-symmetric I-beams. The moment gradient factor,  $C_{mv}$ , also depends on the relative area of web and flange. In the present study, for the evaluation of those previously proposed design equations, the flange area,  $A_f$ , as in the Eq. 8, was taken as the smaller area of the top and bottom flanges for singly-symmetric I-beams. The critical LTB moment of the singly-symmetric unstiffened I-beams investigated in this study was predicted using those equations, labeled as  $M_{cr,predict}$ , and compared against the buckling

moment obtained from the FE analysis,  $M_{cr,FE}$ . The results are normalized by dividing the predicted moment by the FE moment,  $M_{cr,predict}/M_{cr,FE}$ . In this paper, the “design equations” refers to the previously proposed equations by Liang et al. (2022), as shown in Eqs. 6-8.

### 5.1 Unstiffened web under uniform moment (zero shear)

Under the case of uniform moment loading causing zero shear along the unbraced length, the moment gradient factor,  $C_{mv}$ , is taken the value of 1. Fig. 7 summarizes the results for unstiffened beams with various geometries. All the normalized predicted LTB moments were larger than 1, with a maximum value of approximately 1.2, indicating that the proposed equations predicted a larger LTB moment than the FE model. As shown in Fig. 7(b), the normalized predicted buckling moment increased as the effective web slenderness ratio increased, and the predicted capacity was 20% larger than that of the capacity by FE analyses for the slenderest webs. The over-estimation of the LTB capacity was likely due to the LDB effects associated with singly-symmetric I-beams under the case of zero shear which were not considered in the design equations.

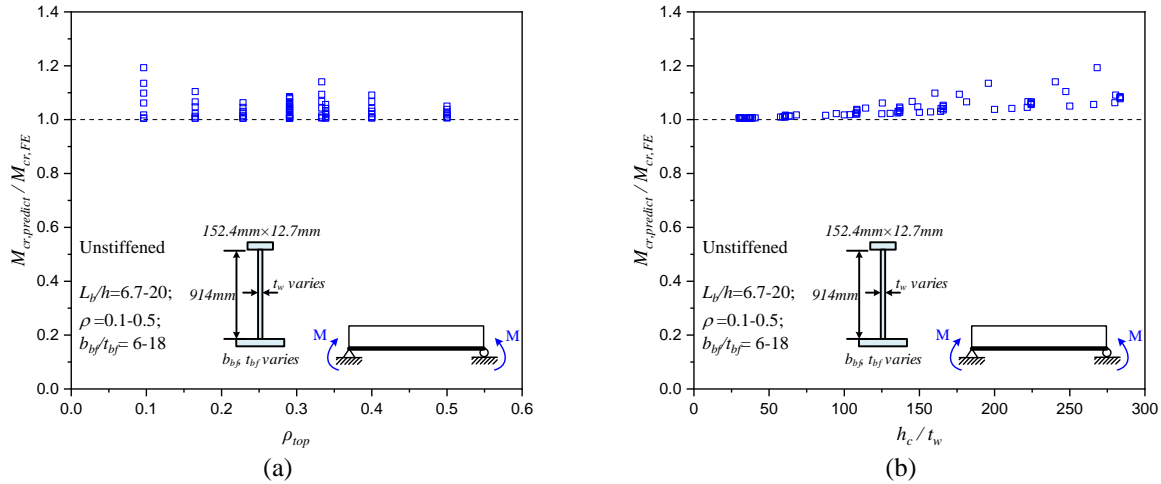


Figure 7: Evaluation of the equations in the case of zero shear with variations in: (a) degree of mono-symmetry; (b) effective web slenderness ratio.

### 5.2 Unstiffened web under constant shear

The feasibility of the design equations was evaluated for unstiffened webs under linearly distributed moment loading causing constant shear along the unbraced length, as shown in Fig. 8. The normalized predicted buckling moment by the equations was in the range of 0.817 to 1.144. The difference between the design results and the FE results increased as the effective web slenderness ratio increased.

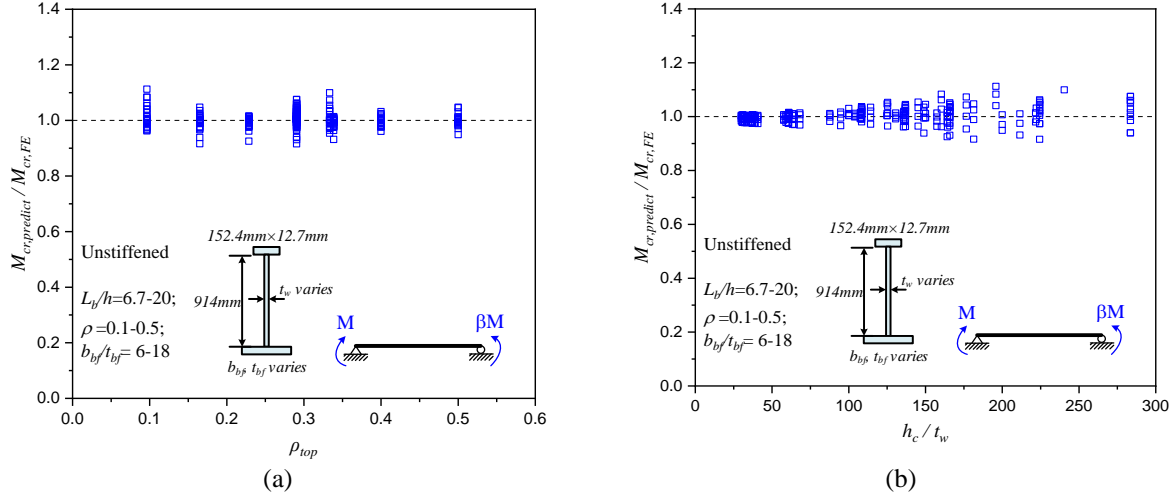


Figure 8: Evaluation of the equations in the case of uniform shear with variations in: (a) degree of mono-symmetry; (b) effective web slenderness ratio.

### 5.3 Unstiffened web under shear gradient

Fig. 9 compares the predicted LTB capacity by the design equations and the eigenvalues obtained from FE analyses in the case of shear gradient. The design equations can provide a relatively accurate prediction of the LTB resistance for singly-symmetric I-beams with compact webs, which is slightly on the conservative side. However, for non-compact and slender webs, which are subjected to more effects of LDB and shear, the design equations can over-estimate or underestimate the LTB capacity for by approximately 20% compared to the FE results.

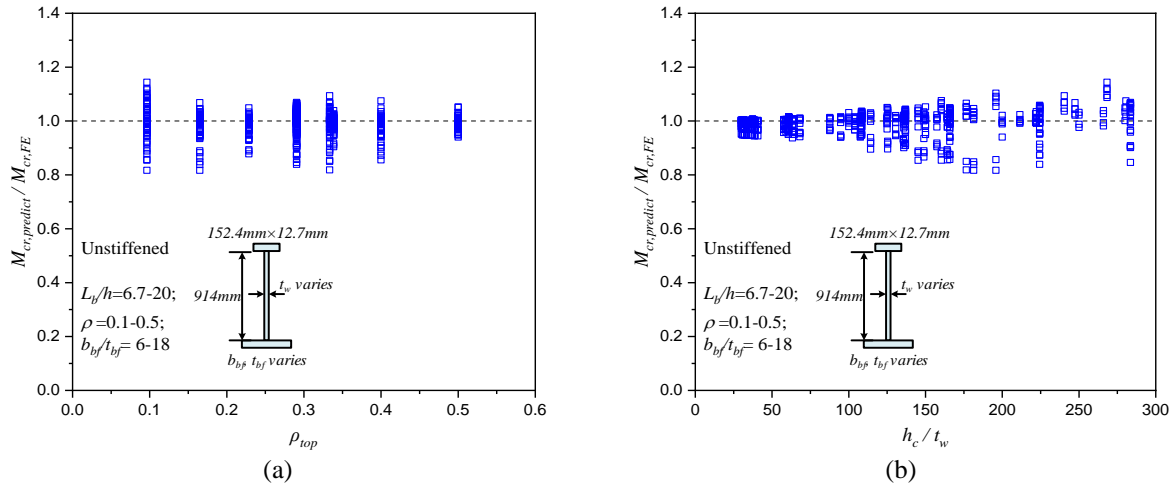


Figure 9: Evaluation of the equations in the case of shear gradient with variations in: (a) degree of mono-symmetry; (b) effective web slenderness ratio.

### 5.4 Partially-stiffened web

The feasibility of the design equations was evaluated for partially-stiffened webs, which had a stiffener spacing-to-depth ratio ( $a/h$ ) in the range of 0.25 to 3.4. Three moment diagrams were considered: 1) unbraced segments of fix-fix beam with UDL; 2) reverse curvature bending; and 3) half of the unbraced segments of fix-fix beam with UDL. Almost all of the predictions of the LTB capacity given by the design equations were on the conservative side compared to the FE results, with a maximum difference of approximately 20%.

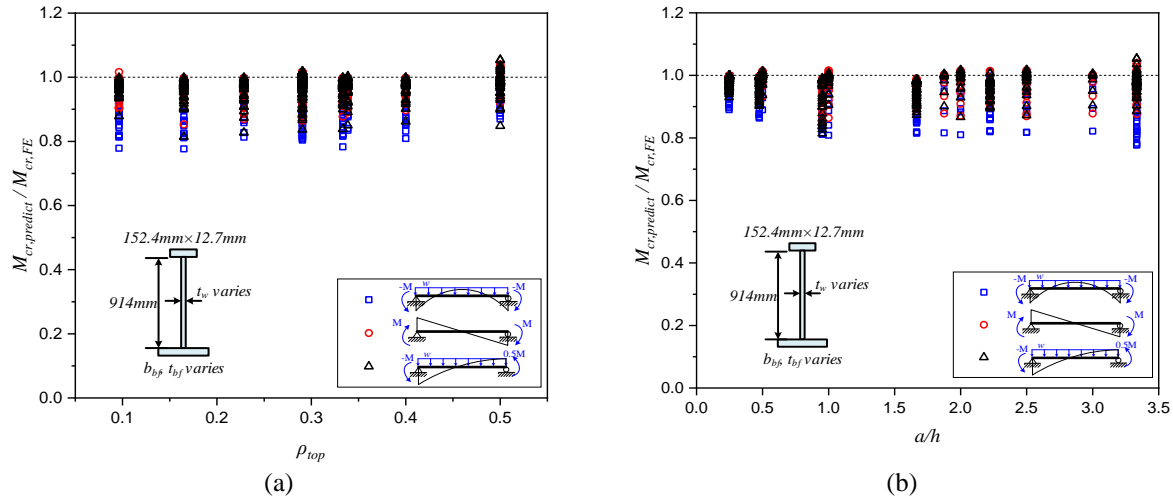


Figure 10: Evaluation of the equations for partially-stiffened webs with variations in: (a) degree of mono-symmetry; (b) stiffened level.

## 6. Conclusions

In this study, numerical parametric studies were performed to investigate the effects of shear on the elastic LTB resistance of singly-symmetric beams through eigenvalue analysis and large-displacement analysis. The effects of the web slenderness ratio, the unbraced length-to-depth ratio, the ratio of top to bottom flange area, and nonlinear geometry on the reduction of the LTB resistance due to shear were evaluated. Previously proposed design equations for doubly-symmetric I-beams were applied to predict the reduction in the LTB for singly-symmetric I-beams and their feasibility was evaluated. The main conclusions and findings are summarized as follows:

- (1) The effective web slenderness ratio plays a significant role in the reduction of the LTB resistance due to shear for singly-symmetric I-beams. The decrease of the unbraced length-to-depth ratio also effectively reduces the negative effects of shear on the LTB capacity. However, the ratio of top to bottom flange area of singly-symmetric sections is not a critical factor for the shear effects on the LTB response.
- (2) The design equations are unconservative in predicting the LTB capacity for singly-symmetric I-beams in the case of zero shear due to the neglect of the LDB effects in the equations. The over-estimation of the LTB is more obvious for webs with higher slenderness ratio for 20%, which are more affected by the LDB effects.
- (3) A maximum of 20% difference was observed between the LTB by design equation and the LTB by FE analyses in the existence of shear along the unbraced length. However, the improvement of the design equations to determine the LTB resistance of singly-symmetric I-beams is needed to have a better fit to the FE results by accounting for the combined effects of LDB and shear.

## References

- AASHTO. (2020). *AASHTO LRFD Bridge Design Specification*. Washington DC: AASHTO.
- AISC. (2016). *Specification for Structural Steel Buildings*. Chicago: AISC.
- Bradford, M.A. (1992). "Lateral-Distortional Buckling of Steel I—Section Members." *Journal of Constructional Steel Research* 23 (1–3): 97–116. [https://doi.org/10.1016/0143-974X\(92\)90038-G](https://doi.org/10.1016/0143-974X(92)90038-G).
- Bradford, Mark A. (1985). "Distortional Buckling of Monosymmetric I-Beams." *Journal of Constructional Steel Research* 5 (2): 123–36. [https://doi.org/10.1016/0143-974X\(85\)90010-0](https://doi.org/10.1016/0143-974X(85)90010-0).
- Bradford, Mark A., and Nicholas S. Trahair. (1981). "Distortional Buckling of I-Beams." *Journal of the Structural Division* 107 (2): 355–70.

- Daley, Aaron J., D. Brad Davis, and Donald W. White. (2017). "Shear Strength of Unstiffened Steel I-Section Members." *Journal of Structural Engineering* 143 (3): 04016190. [https://doi.org/10.1061/\(asce\)st.1943-541x.0001639](https://doi.org/10.1061/(asce)st.1943-541x.0001639).
- Galambos, Theodore V. (1968). *Structural Members and Frames*. Englewood Cliffs, N.J.: Prentice-Hall.
- Helwig, Todd A., Karl H. Frank, and Joseph A. Yura. 1997. "Lateral-Torsional Buckling of Singly Symmetric I-Beams." *Journal of Structural Engineering* 123 (9): 1172–79. [https://doi.org/10.1061/\(ASCE\)0733-9445\(1997\)123:9\(1172\)](https://doi.org/10.1061/(ASCE)0733-9445(1997)123:9(1172)).
- Liang, Chen, Matthew C. Reichenbach, Todd A. Helwig, Michael D. Engelhardt, and Joseph A. Yura. (2022). "Effects of Shear on the Elastic Lateral Torsional Buckling of Doubly Symmetric I-Beams." *Journal of Structural Engineering* 148 (3): 04021301. [https://doi.org/10.1061/\(ASCE\)ST.1943-541X.0003294](https://doi.org/10.1061/(ASCE)ST.1943-541X.0003294).
- Moore, Kevin Spencer. (1995). "Strength of Singly Symmetric Steel Beams with Non-Compact and Slender Compression Elements." MS Thesis, The University of Texas at Austin.
- Phillips, Matthew, Ryan Slein, Ryan J. Sherman, and Donald W. White. (2023). "Experimental Investigation of Doubly-Symmetric Built-up I-Girders Subjected to High Moment Gradient." *Engineering Structures* 283 (August 2022): 115724. <https://doi.org/10.1016/j.engstruct.2023.115724>.
- Reichenbach, Matthew C., Yangqing Liu, Todd A. Helwig, and Michael D. Engelhardt. (2020). "Lateral-Torsional Buckling of Singly Symmetric I-Girders with Stepped Flanges." *Journal of Structural Engineering* 146 (10): 04020203. [https://doi.org/10.1061/\(ASCE\)ST.1943-541X.0002780](https://doi.org/10.1061/(ASCE)ST.1943-541X.0002780).
- Systemes, D. 2020. Abaqus [Computer software].
- Timoshenko, Stephen P., and James M. Gere. (1961). *Theory of Elastic Stability*. New York, NY: McGraw-Hill. <https://asmedigitalcollection.asme.org/appliedmechanics/article/29/1/220/424938/Theory-of-Elastic-Stability-Second-Edition>.
- Winter, George. (1943). "Lateral Stability of Unsymmetrical I-Beams And Trusses in Bending." *Transactions of the American Society of Civil Engineers* 108 (1): 247–60. <https://doi.org/10.1061/TACEAT.0005677>.